Physica A 462 (2016) 783–792

Contents lists available at ScienceDirect

Physica A

journal homepage: www.elsevier.com/locate/physa

Multi-fractal scaling comparison of the Air Temperature and the Surface Temperature over China

Lei Jiang [a,b,*], Jiping Zhang [c], Xinwei Liu [d], Fei Li [e]

[a] School of Marine Sciences, Nanjing University of Information Science and Technology, Nanjing 210044, PR China

[b] Jiangsu Research Center for Ocean Survey Technology, Nanjing 210044, PR China

[c] Beijing Institute of Applied Meteorology, Beijing 100029, PR China

[d] Lanzhou Central Meteorological Observatory, Lanzhou 730020, PR China

[e] Key Laboratory of Watershed Geographic Sciences, Nanjing Institute of Geography and Limnology, Chinese Academy of Sciences, Nanjing 210008, PR China

HIGHLIGHTS

- There exist different multi-fractal phenomena in AT and ST.
- The diversity features of geographic distribution in multi-fractal behaviors.
- Some differences and similarities between AT and ST are successfully detected.

ARTICLE INFO

Article history:
Received 18 January 2016
Received in revised form 19 April 2016
Available online 21 June 2016

Keywords:
Multi-fractal scaling behaviors
MF-DFA
Air Temperature
Surface Temperature

ABSTRACT

The spatial and temporal multi-scaling behaviors between the daily Air Temperature (AT) and the Surface Temperature (ST) over China are compared in about 60-yr observations by Multi-fractal Detrended Fluctuation Analysis (MF-DFA) method. The different fractal phenomena and diversity features in the geographic distribution are found for the AT and ST series using MF-DFA. There are more multi-fractal features for the AT records but less for ST. The respective geographic sites show important scaling differences when compared to the multi-fractal signatures of AT with ST. An interval threshold for 95% confidence level is obtained by shuffling the AT records and the ST records. For the AT records, 93% of all observed stations shows the strong multi-fractal behaviors. In addition, the multi-fractal characteristics decrease with increasing latitude in South China and are obviously strong along the coast. The multi-fractal behaviors of the AT records between the Yangtze River and Yellow River basin and in most regions of Northwest China seem to be weak and not significant, even single mono-fractal features. However, for the ST records, the geographical distributions of multi-fractal phenomenon seem to be in disorder which account for 81% of the stations. The weak multi-fractal behaviors of the ST records are concentrated in North China, most regions of Northeast China.

1. Introduction

As is known to all, there exist Long Range Correlations (LRCs) for the temperature time series [1–7]. Many studies focused on the scaling behaviors of the Air Temperature (AT) and there is only a little research on the scaling behaviors of the Surface

* Corresponding author at: School of Marine Sciences, Nanjing University of Information Science and Technology, Nanjing 210044, PR China.
E-mail address: jianglei@nuist.edu.cn (L. Jiang).

http://dx.doi.org/10.1016/j.physa.2016.06.048
0378-4371/

Temperature (ST) [8]. In fact, the temperature time series show the complex self-similar structures governed by different physical processes containing a variety of temporal–spatial scales. Therefore, it is quite necessary to compare and analyze the multi-fractal scaling behaviors of AT and ST records.

The Detrended Fluctuation Analysis (DFA) method has been introduced to qualify scaling behaviors due to some limitations of traditional methods such as Fourier transform and spectral analysis. The DFA method is established by Peng et al. [9], and extended by Bunde et al. [10]. LRCs have been detected and determined using DFA [11,12]. Kalauzi et al. [13] compared trends and rhythms of complexity climate trends of rainfall data series using fast Fourier transform and fractal dimension. Chelani [14] found the observed extreme CO and NO_2 concentrations are significant in two time scaling regions and the persistence is related with the property of self-organized criticality. Vindel and Polo [15] investigated the relations between the scaling exponents and the orders in the structure functions for the clearness and transmittance indexes. Zhang and Zhao [16] unraveled asymmetric upward and downward long-term persistence analysis in SSTA.

An approach based on the DFA method, called Multi-Fractal Detrended Fluctuation Analysis (MF-DFA), was extended since a mono-fractal scaling behavior cannot fully describe uneven multi-fractal characteristics [17,18]. Multi-fractal theory is a complex self-similar behavior that describes quantitatively the nonlinear evolution and multi-scale characteristics of the system. The MF-DFA method has been successfully applied in many fields [19–21]. Feng et al. [22] analyzed non-universal multi-fractal behaviors of wind speed at four stations over China. Zhang et al. [23] employed three methods to analyze scaling properties of numerically generated series and observed streamflow series. The results show that the average removing method performed reasonably better than the Fourier-based detrending method and adaptive detrending algorithm. Gao and Fu [24] found strong multi-fractal characters over some stations located in the Yunnan, Guangdong, and Inner Mongolia regions by studying the multi-fractal scaling of relative humidity over China.

There are also many studies on multi-fractal characters of temperature time series. Lin et al. [25] characterized different multi-fractal behaviors of temperature over China using a universal model. Du et al. [26] applied the MF-DFA method to determine the thresholds of extreme low minimum and high maximum temperature events. Moreover, the extreme temperature indices are proposed to reflect the severity ranks of extreme temperatures in order to find serious areas of extreme temperature events over Northeast China. Jiang et al. [27] analyzed multi-fractal scaling of four ST records over China and found strong persistence features and different multi-fractal behaviors of ST. In addition, Yuan et al. [28] analyzed the multi-fractal scaling of diurnal temperature range over China. Different multi-fractal characters are found over China taking Yangtze River as the roughly dividing line according to some criterions. Burgueño et al. [29] found that there are no clear spatial distributions for the multi-fractal spectrum parameters of the daily extreme temperatures in Catalonia (NE Spain), but depending on complex self-similar behaviors.

The first aim of this Letter is to study and compare the multi-fractal behaviors and detect the geographical distribution of the scaling law. The paper is organized as follows. In Section 2, the acquisition of the AT and ST records and the MF-DFA method are described. In Section 3, the results of MF-DFA and the multi-fractal spectrum and geographical distributions of multi-fractal strengths are investigated. We summarize the results and draw our conclusions in Section 4.

2. Data and method

2.1. Data records

The high-quality daily surface climatic records including 412 weather stations during the time 1951–2009 are from the Chinese National Meteorological Information Center (NMIC). Many studies have applied the long data records in recent years [25,28]. The daily AT and ST time series are used to study the different scaling behaviors in this paper. The seasonal cycles are removed from the raw data x_i by calculating the AT and ST anomaly $\Delta x_i = x_i - \langle x_i \rangle_d$, $i = 1 \ldots N$, where N is the length of the time series and $\langle x_i \rangle_d$ denotes the average value for a given calendar day.

2.2. The method

The MF-DFA method is mainly described by the following steps [30]. Firstly, the anomaly time series $\{\Delta x_i\}$ are integrated to get the profile. Secondly, the so-called profile is divided into segments of equal length s, and local polynomial fits of order N are computed respectively for each segment υ. Polynomial detrending of order N is capable of eliminating trends up to order $N - 1$. Then calculate the corresponding variance $F^2(\upsilon, s)$ for each segment length s from polynomial fits and take the qth root of the average fluctuation function $F^2(\upsilon, s)^{q/2}$ over all segments. If the time series is long-range power-law correlated, the fluctuation function $F_q(s)$ increases asymptotically with s as power-law: $F_q(s) \sim s^{h(q)}$, where the exponent $h(q)$ describes the scaling behavior of the qth-order fluctuation function. In this Letter, the fourth-order polynomials are used to eliminate cubic trends in the raw data. For stationary series, the exponent $h(2)$ is the well-defined Hurst exponent. For a mono-fractal time series, which can be characterized by a single scaling exponent over all scales, $h(q)$ is independent of the index q, whereas for a multi-fractal time series, $h(q)$ varies with q, which are characterized by more than one scaling exponent indicating multi-fractal behaviors [30].

The singularity spectrum $f(\alpha)$ is also used to characterize multi-fractal scaling behaviors [31,32]. The generalized Hurst exponent $h(q)$ and the scaling exponent $\tau(q)$, the singularity exponent α and the singular spectrum $f(\alpha)$ in multi-fractal

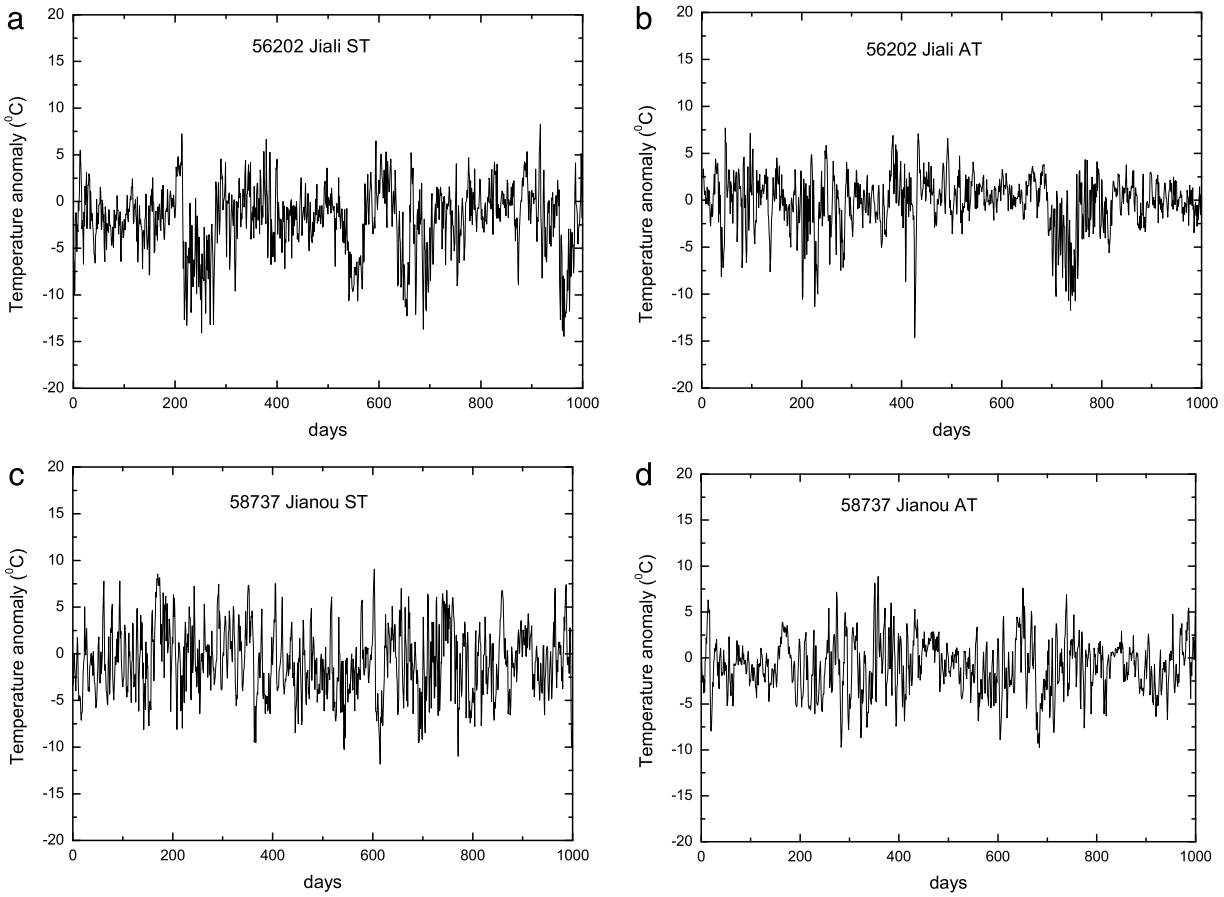

Fig. 1. Temporal variations of the two anomaly ST and AT series about three years. (a) The station Jiali for the ST records in the Tibetan Plateau of China. (b) The analog to (a) but for the AT records. (c) The station Jianou for the ST records in the Southeast of China. (d) The analog to (c) but for the AT records.

Table 1
Co-ordinates of the daily ST and AT time series.

Station num	Name	Lon	Lat	Start–end time
58 737	Jianou	120.12°E	27.20°N	Jan.1953–Dec. 2009
56 202	Jiali	93.17°E	30.40°N	Nov.1954–Dec. 2009

formula have the following relationships via a Legendre transform [31],

$$\tau(q) = qh(q) - 1 \tag{1}$$

$$\alpha(q) = h(q) + qh'(q) \tag{2}$$

$$f(\alpha) = q\alpha - \tau(q) = q[\alpha - h(q)] + 1 \tag{3}$$

where α is the singularity strength, while the singularity spectrum $f(\alpha)$ is characterized by α implies the dimension of the subset of the series.

3. Results

As two representative examples, Table 1 provides the co-ordinates of the map of the station Jiali in the Tibetan Plateau of China and the station Jianou in the Southeast of China. Fig. 1(a)–(d) show three years of the anomaly ST and AT time series for stations Jiali and Jianou, respectively. It can be seen that the fluctuations of the time series are different for different climate variables. For station Jiali, the fluctuation of the ST record appears more furious than that of the AT record, whereas for station Jianou, the fluctuation seems to appear the opposite case. But for both stations, the AT and ST time series are characterized by the bursts of high-frequency fluctuations and reflect complicated dynamic characteristics.

The profiles of the daily ST and AT records for two stations exhibit similar variation trends in Fig. 2(a)–(d) (black solid lines) on the whole. The profiles of the ST records decrease below the value 0 till the time scale is about 7000 days and then

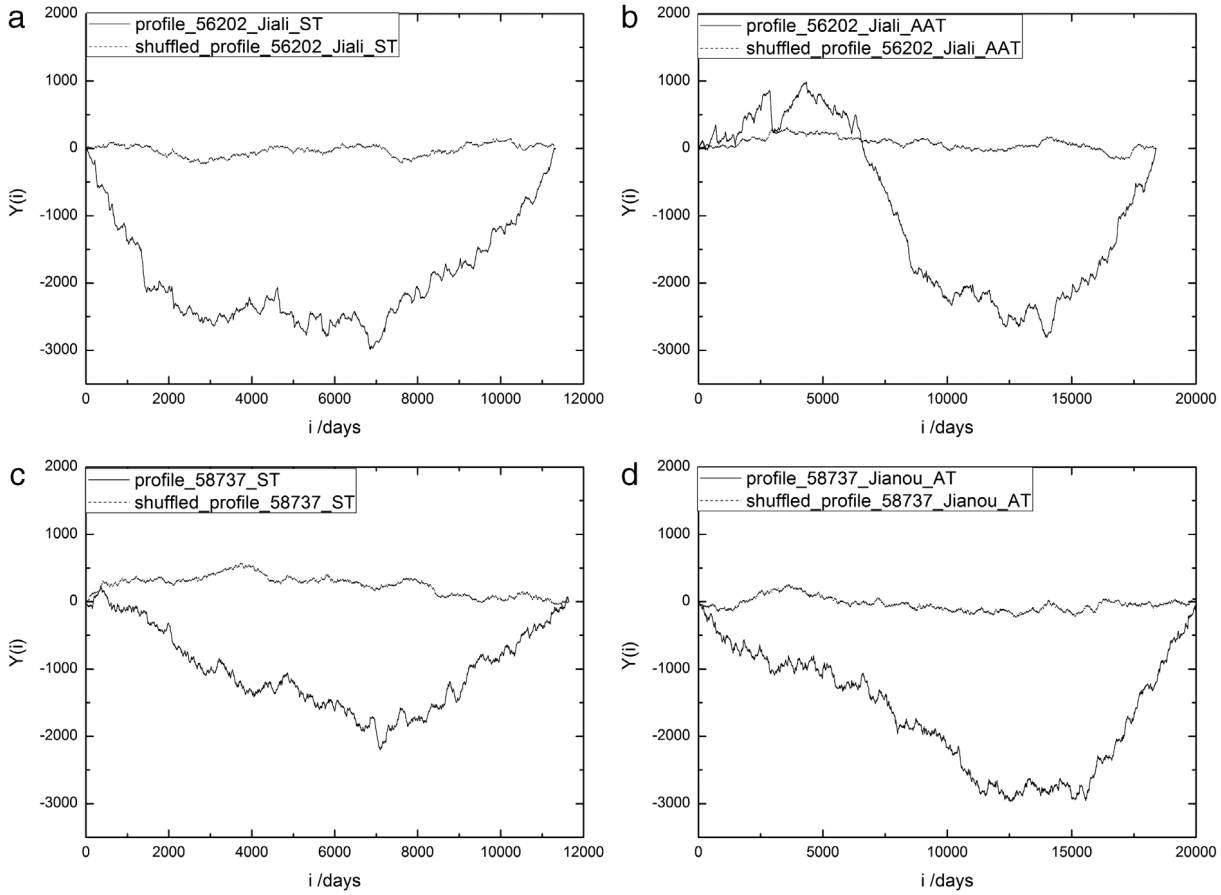

Fig. 2. The profiles of the two anomaly ST and AT series for stations Jiali and Jianou. (a) The black solid line represents the profile of the ST records for station Jiali; The black dash line represents the profile of the shuffled data. (b) The analog to (a) but for the AT records. (c) The profile of the ST records for station Jianou. (d) The analog to (c) but for the AT records.

increase, taking on a shape just like the letter "v" in Fig. 2(a) and (c). However, there is a slight difference for the AT records. The profile for station Jiali firstly fluctuates above the value 0 and then decreases till the value of the profile is smaller than −2500. Furthermore, we remove the trends and correlations by randomly shuffling the ST and AT data sets in order to test the long-range correlations. Fig. 2(a)–(d) (black dash lines) represent the profiles of the shuffled series for the above two stations, respectively. It is obvious that the profiles of the ST and AT time series over stations Jiali and Jianou are close to 0 just as expected.

Next, we applied the method of MF-DFA4 (actually, different order MF-DFA show the similar results and eliminate the possible nonlinear trends, here the fourth-order MF-DFA4 is used to analyze the data records in this paper) to the anomaly time series. The fluctuation functions $F_q(s)$ are calculated by using MF-DFA4. Fig. 3(a)–(d) show the log–log plots of the fluctuation functions with varying moments ($q = 5, 4, 3, 2, 1, -1, -2, -3, -4, -5$). For station Jiali, the curve slopes of the ST record become steeper and steeper from the bottom to the top, whereas the curve slopes of the AT record change little. For station Jianou, the variation of the curve slopes for the AT and ST records are on the opposite. In order to calculate the index q dependence of the slopes $h(q)$, we selected the asymptotic long-range power-law correlations in the range 300–1000 days, where the scaling behavior is more or less constant for different q. Fig. 3(e)–(h) show the generalized Hurst exponents $h(q)$ with varying moments ($q = 5, 4, 3, 2, 1, -1, -2, -3, -4, -5$) respectively. The exponents $h(q)$ decrease with the increase of the moment q which indicate the presence of the strong multi-fractal behavior in ST series for station Jiali and in AT series for station Jianou. However, the exponents $h(q)$ change little with the increase of the moment q in AT series for station Jiali and in ST series for station Jianou indicating the weak multi-fractal behavior. By randomizing shuffled surrogates of the MF-DFA4 results, as shown in Fig. 4(a)–(d), we find the origin of multi-fractality is from long-range correlations, not from a broad probability density function of time series. Fig. 4(e)–(h) show that the exponents $h(q)$ with varying moments ($q = 5, 4, 3, 2, 1, -1, -2, -3, -4, -5$) are close to about 0.5 as random time series.

According to the formula (1)–(3), the singularity strength α and the multi-fractal spectrum $f(\alpha)$ can be calculated by the exponents $h(q)$ [31,32]. Fig. 5(a)–(d) show the singularity spectra of the AT and ST records for stations Jiali and Jianou. It is shown that the widths of multi-fractal spectrum are very different indicating the non-universality of the multi-fractal

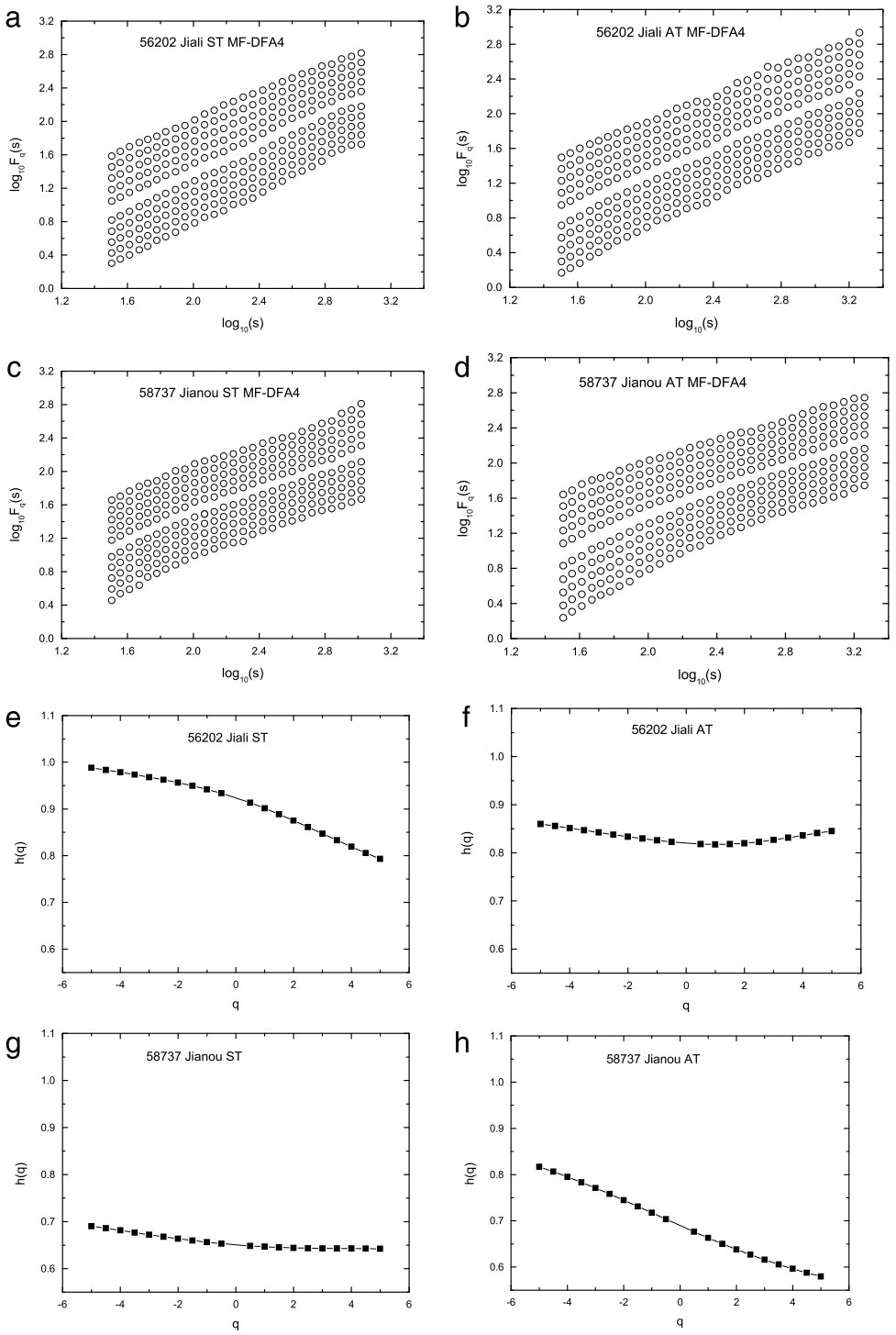

Fig. 3. (a) Double log plots of the MF-DFA4 curves of the ST records for the station Jiali. From the top to the bottom curves correspond to different q (from $q = 5$ to $q = +5$). (b), (c) and (d) The analog to (a) but the AT records, the ST records for station Jianou, and the AT records for station Jianou. (e) $h(q)$ vs. q plots for Jiali. Solid squares: obtained from MF-DFA4 results in (a). (f), (g) and (h) The analog to (e) but the AT records, the ST records for station Jianou, and the AT records for station Jianou.

behaviors. The singularity spectrum, approximately an upside-down parabola, shows similar shapes in Fig. 5(a) and (d). It can be considered that the singularity spectrum exhibits strong multi-fractal properties. And the multi-fractal characteristics are mainly due to the difference between LRCs of the large fluctuation and the small fluctuation. Comparing Fig. 5(a) with

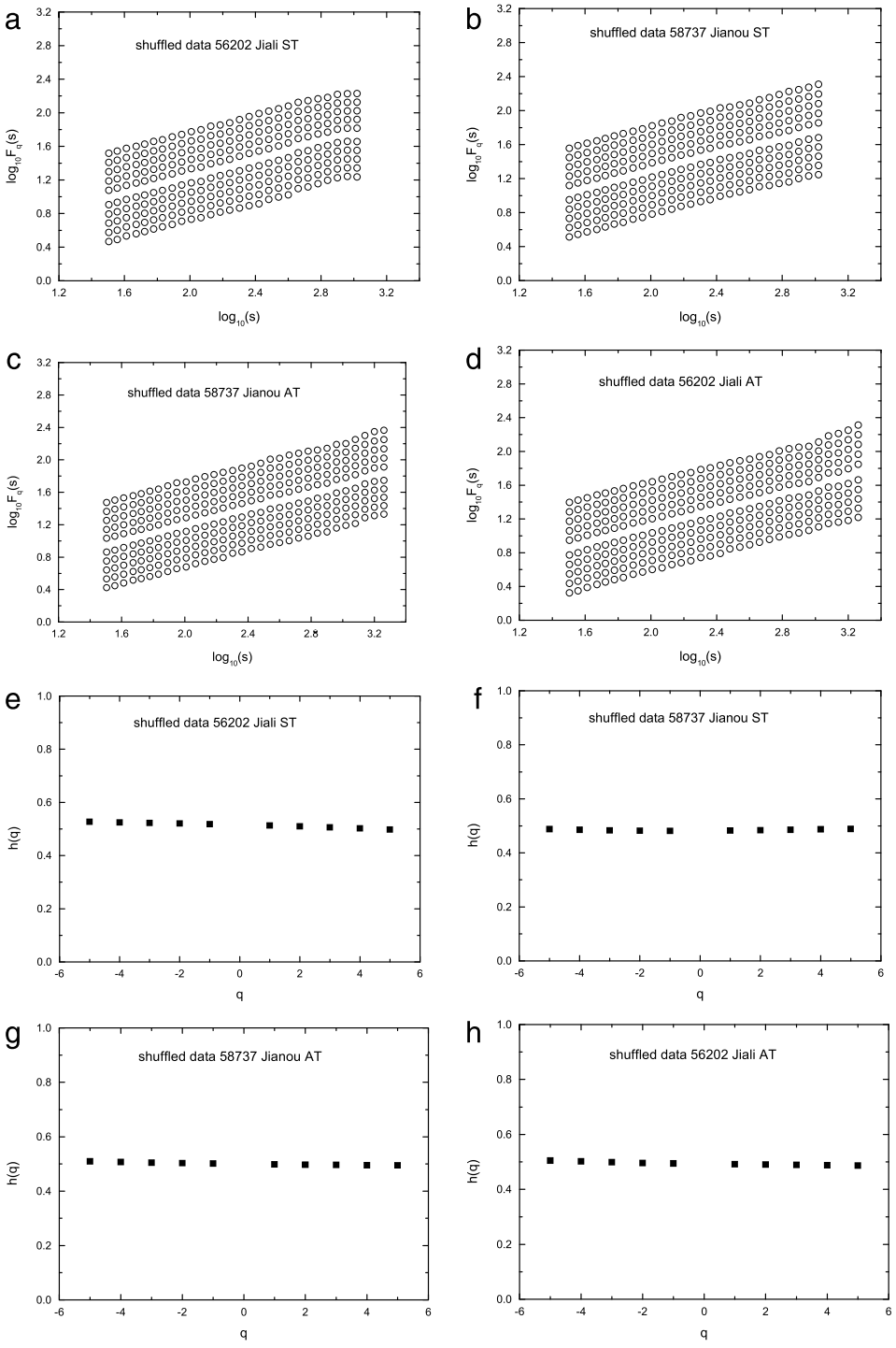

Fig. 4. (a) Double log plots of the MF-DFA4 curves of the shuffled ST records for the station Jiali. From the top to the bottom curves correspond to different q (from $q = 5$ to $q = +5$). (b), (c) and (d) The analog to (a) but the shuffled AT records, the shuffled ST records for station Jianou, and the shuffled AT records for station Jianou. (e) The shuffled $h(q)$ vs. q plots for station Jiali. Solid squares: obtained from MF-DFA4 results in (a). (f), (g) and (h) but the shuffled AT records, the shuffled ST records for station Jianou, and the shuffled AT records for station Jianou.

(b), the memory time of ST is longer than that of AT at Jiali station, but reversed at Jianou station. This may be caused by the complexity of the physical process in controlling the temperature variation, such as their location dependence. The strong multi-fractal behavior implies more obvious nonlinear fluctuation. Furthermore, the asymmetry of the singular spectrum reflects the ranges of variation in scaling exponents caused by large or small fluctuations. From Fig. 5(a) and (d) we can see

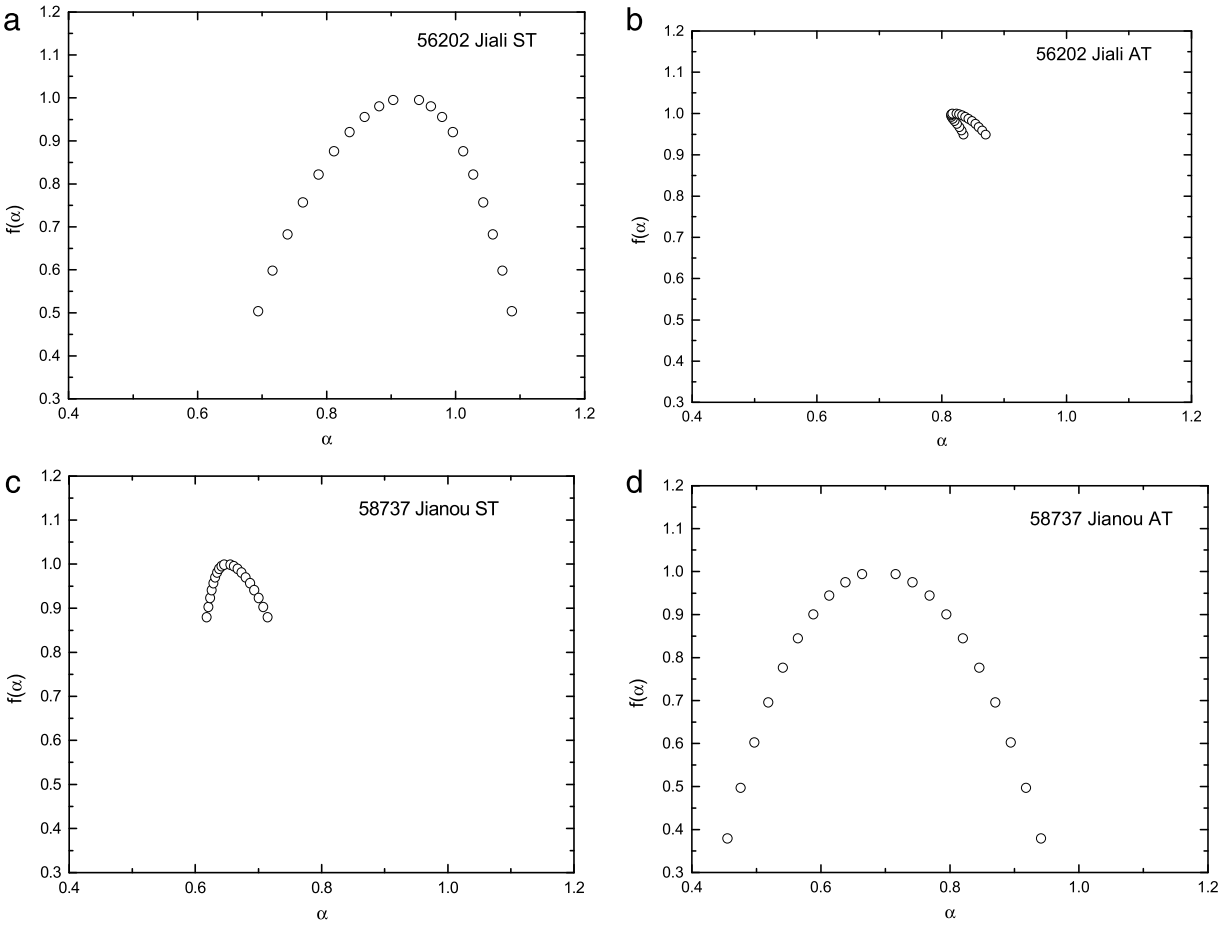

Fig. 5. (a) The multi-fractal spectra $f(\alpha)$ for the ST record of station Jiali. (b), (c) and (d) The analog to (a) but the AT records, the ST records for station Jianou, and the AT records for station Jianou.

Table 2
Statistical comparisons of the daily ST and AT time series.

Name	Mean	Standard deviation	Minimum	Maximum
AT	0.19	0.13	−0.06	0.6
ST	0.09	0.08	−0.31	0.31

that the singular spectra of ST at the Jiali station and AT at the Jianou station are symmetrical indicating that the ranges of LRCs caused by large and small fluctuations of the temperature time series are equivalent. By contrast, the widths of the spectrum in Fig. 5(b) and (c) are narrow exhibiting the weak multi-fractal behaviors, even the mono-fractal phenomenon. The singular spectrum will become a point if the time series is completely mono-fractal. Thus, next we pay close attention to the multi-fractal scaling differences of the AT and ST records for different weather stations over China.

Because $h(+5)$ represents the scaling behavior of largest fluctuation and $h(-5)$ reflects the scaling behavior of minimum fluctuation, their difference reflects the multi-fractal phenomenon. Therefore, the strength of the multi-fractal behavior can be characterized by the difference of the asymptotical values of $h(q)$, namely $\Delta h = h(-5) - h(+5)$. The frequency distributions of Δh for ST and AT shown in Fig. 6 are obviously distinguished, where the histogram of Δh for ST is symmetrically distributed, but for AT it is shifted positively. The histogram of Δh for AT does not exhibit well-developed Gaussian shape. Large fractal indexes occupy a dominant position, and the range of scaling exponent caused by small fluctuation for AT is larger, which reflects that small fluctuation is more complex than large fluctuation. The average, standard deviation, minimum and maximum values of the AT and ST records for all 412 weather stations are shown in Table 2, which also confirms non-Gaussian shape for AT. The differences of the AT and ST records show non-universal characteristics over China. More multi-fractal features are found for AT but less for ST.

In order to verify the multi-fractal feature, we shuffle the ST and AT data records. An interval threshold of 95% confidence level is obtained from the probability density distribution of shuffled ST and AT time series. The ranges of the interval threshold are from −0.03 to 0.04 for 95% confidence level. According to above interval threshold, the geographical

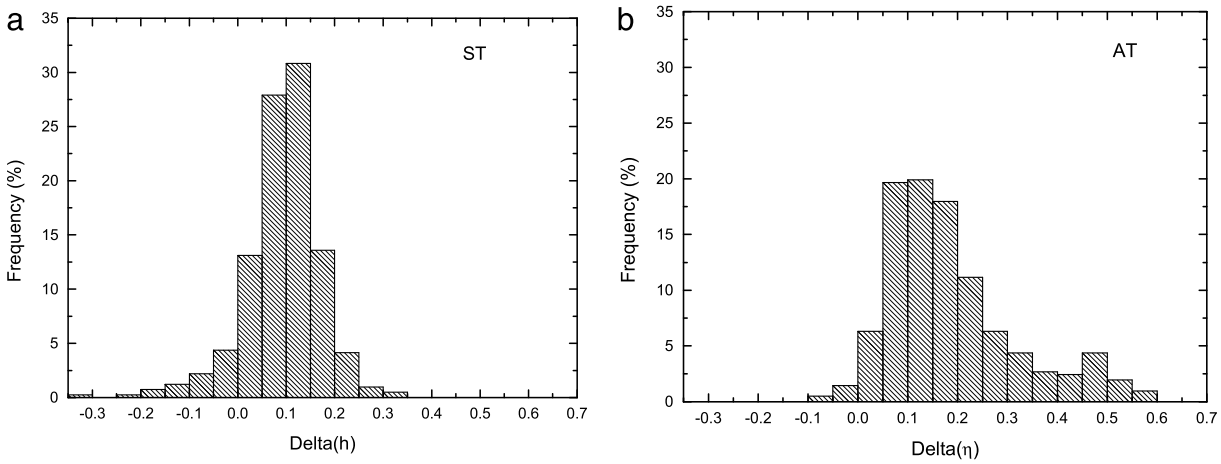

Fig. 6. The histograms of Δh of the ST and AT series for 412 weather stations over China. (a) The ST series. (b) The AT series.

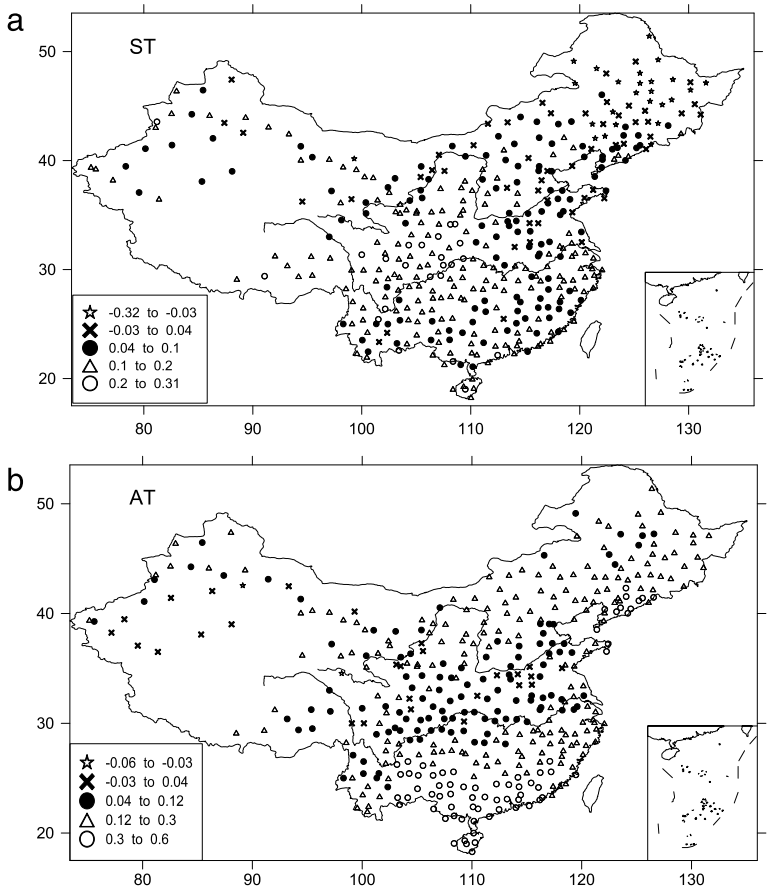

Fig. 7. The geographical distributions of Δh of the ST and AT series for 412 weather stations over China. (a) The ST series. (b) The AT series.

distributions of Δh for the ST and AT records are shown in Fig. 7(a) and (b). It can be seen that there are the different multi-fractal characteristics between ST and AT.

On the one hand, the ST records have strong multi-fractal behaviors accounting for 81% of all meteorological observation stations located in most of China. The strong multi-fractal behaviors are mainly concentrated in the upstream areas between Yangtze River and Yellow River and along the Yangtze River Basin. In contrast, the weak multi-fractal behaviors are mainly concentrated in some areas of North China. An interesting finding is that the values of Δh are smaller than -0.03 in most regions of Northeast China. In fact, the spatial distributions of ST do not have obvious regularities. This is likely to reflect

the complexity and location dependences of climate change over China. On the other hand, for the AT records, about 7% of weather stations exhibit the weak multi-fractal behavior and are mainly located in the areas between the Yangtze River and Yellow River basin and in some regions of Northwest China, i.e. $\Delta h \approx -0.03 \sim 0.04$. Similar result has been reported in the [25]. It must be noted, however, that other stations located in most regions of South China and North China, where the AT records appear to be more nonlinear and singular than that in other places over China, show the strong multi-fractal behaviors, i.e. Δh above the value 0.04, which account for 93% of all sites almost covered all areas of China. Furthermore, the multi-fractal characteristics of AT vary obviously with latitude and decrease with increasing latitude in South China. Moreover, the values of Δh are also relatively high along the coast line. In general, the different geographic stations show important scaling differences when their multi-fractal behaviors of the AT and ST records are compared. The differences of the multi-fractal behaviors are probably caused by the different climatic conditions around the different weather stations. The specific physical mechanisms need to be studied further.

4. Conclusion and discussions

In this letter, we have compared and analyzed the different multi-fractal behaviors of the daily AT and ST records from 412 weather stations over China using the MF-DFA method. Some differences and similarities between sites were successfully detected. We found that the AT and ST records exhibit the different mono- and multi-fractal behaviors, whereas, the strength of the multi-fractal behaviors appears non-universal over China.

There are the high-frequency fluctuations for the AT and ST time series which imply the complex dynamical behaviors. The curve slopes of AT and ST are constant or different with different moments q indicating mono- and multi-fractal behaviors. Meanwhile, the singularity spectra of AT and ST also exhibit different fractal properties. The width ranges of the singularity spectra show the strong or weak multi-fractal behaviors, even the mono-fractal characteristics.

The frequency histogram of Δh for ST is symmetrically distributed and can be characterized by a well-developed Gaussian shape, but for AT does not exhibit well-developed Gaussian shape which shifts positively. For AT, small fluctuation is more complex than large fluctuation, however the feature is reversed for ST.

We obtain an interval threshold of 95% confidence level by shuffling the ST and AT data records and take the same threshold from -0.03 to 0.04 as the interval. The spatial distributions of Δh show different location dependences of multi-fractal characteristics for ST and AT. On the whole, 81% of all stations for ST and 93% of all sites for AT display multi-fractal behaviors. The multi-fractal features for AT decrease with increasing latitude in South China and are strong along the coastline. There are no obvious regularities for ST.

Comparing the multi-fractal behaviors of AT with that of ST, there exist obvious scaling differences at different weather stations. The reasons why the spatial distributions of multi-fractal behaviors for AT and ST have significant differences are diverse. This may be caused by the different terrain, land–sea difference and climatic conditions. The physical mechanisms will be investigated and analyzed further.

Acknowledgments

Many thanks are due to supports from the Startup Foundation for Natural Science Foundation of Jiangsu Province (BK20151060), the Strategic Priority Research Program of the Chinese Academy of Sciences (XDA11010102), 973 project (2012CB956001), the 2015 Jiangsu Program of Entrepreneurship and Innovation Group, Introducing Talent of NUIST (2014r18). The authors also express their great appreciation to the editor and the anonymous referees for their valuable suggestions.

References

[1] P. Talkner, R.O. Weber, Power spectrum and detrended fluctuation analysis: Application to daily temperatures, Phys. Rev. E. 62 (1) (2000) 150.
[2] R.B. Govindan, D. Vyushin, A. Bunde, S. Brenner, S. Havlin, H.J. Schellnhuber, Global climate models violate scaling of the observed atmospheric variability, Phys. Rev. Lett. 89 (2) (2002) 028501.
[3] F. Klaus, R. Blender, Scaling of atmosphere and ocean temperature correlations in observations and climate models, Phys. Rev. Lett. 90 (10) (2003) 108501.
[4] M.L. Kurnaz, Application of detrended fluctuation analysis to monthly average of the maximum daily temperatures to resolve different climates, Fractals 12 (04) (2004) 365–373.
[5] A. Király, I.M. Jánosi, Detrended fluctuation analysis of daily temperature records: geographic dependence over Australia, Meteorol. Atmos. Phys. 88 (3–4) (2005) 119–128.
[6] N. Yuan, Z. Fu, J. Mao, Different scaling behaviors in daily temperature records over China, Physica A 389 (19) (2010) 4087–4095.
[7] L. Jiang, N. Yuan, Z. Fu, D. Wang, X. Zhao, X. Zhu, Subarea characteristics of the long range correlations and the index χ for daily temperature records over China, Theor. Appl. Climatol. 109 (1–2) (2012) 261–270.
[8] L. Jiang, N. Li, Z. Fu, J. Zhang, Long-range correlation behaviors for the 0-cm average ground surface temperature and Air Temperature over China, Theor. Appl. Climatol. 119 (1–2) (2015) 25–31.
[9] C.-K. Peng, S.V. Buldyrev, S. Havlin, M. Simons, H.E. Stanley, A.L. Goldberger, Mosaic organization of DNA nucleotides, Phys. Rev. E 49 (2) (1994) 1685.
[10] A. Bunde, S. Havlin, J.W. Kantelhardt, T. Penzel, J.H. Peter, K. Voigt, Correlated and uncorrelated regions in heart-rate fluctuations during sleep, Phys. Rev. Lett. 85 (17) (2000) 3736–3739.
[11] K. Ivanova, M. Ausloos, Application of the detrended fluctuation analysis (DFA) method for describing cloud breaking, Physica A 274 (1) (1999) 349–354.
[12] X. Chen, G.X. Lin, Z.T. Fu, Long-range correlations in daily relative humidity fluctuations: A new index to characterize the climate regions over China, Geophys. Res. Lett. 34 (7) (2007) L07804.

[13] A. Kalauzi, M. Cukic, H. Millán, S. Bonafoni, R. Biondi, Comparison of fractal dimension oscillations and trends of rainfall data from Pastaza Province, Ecuador and Veneto, Italy, Atmos. Res. 93 (4) (2009) 673–679.
[14] A.B. Chelani, Persistence analysis of extreme CO, NO_2 and O_3 concentrations in ambient air of Delhi, Atmos. Res. 108 (2012) 128–134.
[15] J.M. Vindel, J. Polo, Intermittency and variability of daily solar irradiation, Atmos. Res. 143 (2014) 313–327.
[16] W.F. Zhang, Q. Zhao, Asymmetric long-term persistence analysis in sea surface temperature anomaly, Physica A 428 (2015) 314–318.
[17] K. Hu, P.C. Ivanov, Z. Chen, P. Carpena, H.E. Stanley, Effect of trends on detrended fluctuation analysis, Phys. Rev. E 64 (1) (2001) 011114.
[18] J.W. Kantelhardt, E. Koscielny-Bunde, H.A. Rego, S. Havlin, A. Bunde, Detecting long-range correlations with detrended fluctuation analysis, Physica A 295 (3) (2001) 441–454.
[19] K. Matia, Y. Ashkenazy, H.E. Stanley, Multifractal properties of price fluctuations of stocks and commodities, Europhys. Lett. 61 (3) (2003) 422.
[20] R.G. Kavasseri, R. Nagarajan, A multi-fractal description of wind speed records, Chaos Solitons Fractals 24 (1) (2005) 165–173.
[21] N.K. Vitanov, E.D. Yankulova, Multi-fractal analysis of the long-range correlations in the cardiac dynamics of Drosophila melanogaster, Chaos Solitons Fractals 28 (3) (2006) 768–775.
[22] T. Feng, Z.T. Fu, X. Deng, J.Y. Mao, A brief description to different multi-fractal behaviors of daily wind speed records over China, Phys. Lett. A 373 (45) (2009) 4134–4141.
[23] Q. Zhang, Y. Zhou, V.P. Singh, Y.D. Chen, Comparison of detrending methods for fluctuation analysis in hydrology, J. Hydrol. 400 (1) (2011) 121–132.
[24] L.H. Gao, Z.T. Fu, Multi-fractal behaviors of relative humidity over China, Atmos. Ocean. Sci. Lett. 6 (2) (2013) 74–78.
[25] G.X. Lin, Z.T. Fu, A universal model to characterize different multi-fractal behaviors of daily temperature records over China, Physica A 387 (2) (2008) 573–579.
[26] H.B. Du, Z.F. Wu, M. Li, Y.H. Jin, S.W. Zong, X.J. Meng, Characteristics of extreme daily minimum and maximum temperature over Northeast China, 1961–2009, Theor. Appl. Climatol. 111 (1–2) (2013) 161–171.
[27] L. Jiang, X. Zhao, N.N. Li, F. Li, Z.Q. Guo, Different multi-fractal scaling of the 0-cm average ground surface temperature of four representative weather stations over China, Adv. Meteorol. 2013 (2013) (2013) 341934.
[28] N.M. Yuan, Z.T. Fu, J.Y. Mao, Different multi-fractal behaviors of diurnal temperature range over the north and the south of China, Theor. Appl. Climatol. 112 (3–4) (2013) 673–682.
[29] A. Burgueño, X. Lana, C. Serra, M.D. Martínez, Daily extreme temperature multifractals in Catalonia (NE Spain), Phys. Lett. A 378 (11) (2014) 874–885.
[30] J.W. Kantelhardt, S.A. Zschiegner, E. Koscielny-Bunde, S. Havlin, A. Bunde, H.E. Stanley, Multifractal detrended fluctuation analysis of nonstationary time series, Physica A 316 (1) (2002) 87–114.
[31] J. Feder, Fractals, Plenum Press, New York, 1988.
[32] A. Bunde, S. Havlin, Fractals in Science, Springer-Verlag, Heidelberg, 1995.